

Structural and vibrational properties of $(\text{Si})_4/(\text{Ge})_4$ superlattices

Zi Jian

Department of Physics, Fudan University, Shanghai 200 433, People's Republic of China

Zhang Kaiming and Xie Xide

Chinese Center of Advanced Science and Technology (World Laboratory), P.O. Box 8730,

Beijing 100 080, People's Republic of China

and Department of Physics, Fudan University, Shanghai 200 433, People's Republic of China

(Received 5 January 1990)

The structural and vibrational properties of a strained $(\text{Si})_4/(\text{Ge})_4$ superlattice grown on a (001)-oriented $\text{Si}_{1-x}\text{Ge}_x$ ($0 \leq x \leq 1$) substrate are studied. The geometries of the strained superlattice for different substrates are obtained. The calculations show that with proper choice of x (0.46) the symmetrically strained $(\text{Si})_4/(\text{Ge})_4$ superlattice can be obtained, yielding large superlattice thickness. The strains are taken into account in the investigations of lattice dynamics of the superlattice. Phonon spectra of the superlattice grown on a Si substrate and phonon frequency shifts induced by strain are discussed.

I. INTRODUCTION

The possibility of combining and manipulating materials to obtain new materials that share the advantageous properties of the constituent materials has generated much interest. In the growth of superlattices, controlled variation of the composition, strain, and thickness of the layers provides electronic, optical, and dynamical properties unlike any ordinary bulk material.¹ Despite the large lattice mismatch (4%) between Si and Ge, ultrathin superlattices consisting of these materials have now been grown by molecular-beam epitaxy (MBE).²⁻⁸ The growth of Ge up to six layers pseudomorphically restricted to a Si(100) substrate has been achieved by Pearsall *et al.*⁷ More important is the fact that direct optical transitions in $(\text{Si})_4/(\text{Ge})_4$ superlattices grown on a Si(001) substrate are observed, which has been an encouraging step towards making significant improvements in the electronic properties of Si. Recently much attention has been paid to the electronic properties of Si/Ge superlattices with the hope of obtaining a direct-band-gap superlattice.⁹⁻¹²

The vibrational properties of Si/Ge superlattices have also been extensively studied both experimentally²⁻⁸ and theoretically.¹³⁻¹⁵ Because of its conceptual simplicity and the possibility of a straightforward interpretation of the experimental data, one-dimensional models for Si/Ge superlattices have been extensively used.¹²⁻¹⁴ Only recently, three-dimensional calculations of phonon spectra have appeared.¹⁵ The large lattice mismatch (4%) between Si and Ge, which affects the electronic and vibrational properties of superlattices, can be completely accommodated by the lattice strain in the commensurate or pseudomorphous Si/Ge layers. The strain was taken into consideration in current studies of electronic structures of Si/Ge superlattices grown on certain substrates.¹⁰⁻¹² However, in many lattice-dynamics calculations,¹³⁻¹⁵ detailed structural configurations of superlattices have not

been taken into account. In order to understand further details of the electronic and dynamical properties of superlattices, the structural configurations of strained superlattices must be investigated.

Generally, strain varies with the substrate selected. Many experimental and theoretical studies have been carried out with (001)-oriented Si substrate. Detailed band-structure calculations have shown that⁹⁻¹² the nature of the lowest electronic transitions depends considerably on the lattice constant to which the superlattices are strained, i.e., on the substrate selected. However, a more preferable superlattice $(\text{Si})_4/(\text{Ge})_4$ might be grown on an alloy substrate $\text{Si}_{1-x}\text{Ge}_x$. Naturally, the choice of the substrate is of equal importance for the phonon spectra of strained Si/Ge superlattices. In the present work, geometrical structures and vibrational properties of strained $(\text{Si})_4/(\text{Ge})_4$ superlattices are investigated on different (001)-oriented alloy substrate $\text{Si}_{1-x}\text{Ge}_x$ with x ranging from 0 to 1. The Keating model¹⁶ is adopted to describe the elastic strain energy of the superlattice. The structures of the superlattice are then determined by minimization of the elastic strain energy. In Sec. II the Keating model and parameters used are discussed. The structural configurations of $(\text{Si})_4/(\text{Ge})_4$ superlattices are presented in Sec. III and the favorable substrate for the growth of $(\text{Si})_4/(\text{Ge})_4$ superlattices is given in Sec. IV. The vibrational properties are discussed in Sec. V, and Sec. VI gives discussion and conclusion.

II. KEATING MODEL

The Keating model¹⁶ has been widely used to describe the elastic energy of covalent crystals with zinc-blende structure for studying elastic^{16,17} and structural¹⁸⁻²² properties. The elastic energy described by the Keating model¹⁶ is given by

$$E = \sum_{R,R'} \alpha(s,s') (\mathbf{X}_{ss'} \cdot \mathbf{X}_{ss'} - r_0^2)^2 + \sum_{R,R',R''} \beta(s,s',s'') (\mathbf{X}_{ss'} \cdot \mathbf{X}_{ss''} + \frac{1}{3} r_0^2)^2, \quad (1)$$

where $\mathbf{X}_{ss'} = \mathbf{X}_s - \mathbf{X}_{s'}$ is the position vector between atom s and atom s' and r_0 is the equilibrium bond length. The factor $\frac{1}{3}$ in the second term gives a tetrahedral equilibrium bond configuration. The first sum is taken over all nearest-neighbor bonds and $\alpha(s,s')$ describes the site-dependent bond-stretching interaction between atom s and atom s' . The second sum is taken over all nearest-neighbor bond pairs and $\beta(s,s',s'')$ is the site-dependent force constant governing the bond-bending interaction between bond vector $\mathbf{X}_{ss'}$ and $\mathbf{X}_{ss''}$. The values of parameters α and β used in the present paper are given in Table I. The values of Keating parameters for Ge are taken from Ref. 17, while the parameters for Si are taken from Ref. 15. These parameters give good descriptions of lattice dynamics for both Si and Ge. By using these values of α and β , Alonso *et al.*¹⁵ studied lattice dynamics of Si/Ge superlattices without taking strain into consideration. In the case of a structure with more than one kind of atom in a unit cell, Eq. (1) should be changed to¹⁸

$$E = \sum_{R,R'} \alpha(s,s') [\mathbf{X}_{ss'} \cdot \mathbf{X}_{ss'} - (b_s + b_{s'})^2]^2 + \sum_{R,R',R''} \beta(s,s',s'') [\mathbf{X}_{ss'} \cdot \mathbf{X}_{ss''} + \frac{1}{3} (b_s + b_{s'}) (b_s + b_{s''})]^2, \quad (2)$$

where b_s is the covalent radius of atom s . In the present calculations, for Si/Ge superlattices, the Keating parameters α and β near the interface Si-Ge are determined by

$$\alpha(\text{SiGe}) = \frac{1}{2} [\alpha(\text{SiSi}) + \alpha(\text{GeGe})], \quad (3a)$$

$$\beta(\text{SiGeSi}) = \beta(\text{GeSiGe}) = \frac{1}{2} [\beta(\text{SiSiSi}) + \beta(\text{GeGeGe})], \quad (3b)$$

$$\beta(\text{SiSiGe}) = \frac{1}{3} [2\beta(\text{SiSiSi}) + \beta(\text{GeGeGe})], \quad (3c)$$

$$\beta(\text{SiGeGe}) = \frac{1}{3} [\beta(\text{SiSiSi}) + 2\beta(\text{GeGeGe})]. \quad (3d)$$

In the lattice-dynamical calculations of Alonso *et al.*,¹⁵ all the values of $\beta(\text{SiGeSi})$, $\beta(\text{SiSiGe})$, and $\beta(\text{SiGeGe})$ are assumed to take the average of $\beta(\text{SiSiSi})$ and $\beta(\text{GeGeGe})$. In the recent *ab initio* calculations of Froyen *et al.*,¹⁰ it was found that the differences between these parameters are quite significant. The parameters deduced from Eq. (3) seem to be more reasonable than those from Ref. 15 with respect to the results obtained by Froyen *et al.*¹⁰

TABLE I. Values of the Keating parameters α and β (in units of $\text{eV}/\text{\AA}^4$) for Si and Ge.

	α ($\text{eV}/\text{\AA}^4$)	β ($\text{eV}/\text{\AA}^4$)
Si ^a	0.1851	0.0488
Ge ^b	0.1508	0.0443

^a Reference 15.

^b Reference 17.

III. STRUCTURAL PROPERTIES OF A $(\text{Si})_4/(\text{Ge})_4$ SUPERLATTICE

The (001)-oriented $(\text{Si})_4/(\text{Ge})_4$ superlattice is studied in a tetragonal unit cell consisting of four atoms from each constituent. This is illustrated in Fig. 1. Growth on different kinds of substrates $\text{Si}_{1-x}\text{Ge}_x$ ($0 \leq x \leq 1$) is considered in our calculations. When $x=0$, the corresponding substrate is Si, and when $x=1$, the substrate is Ge. It is assumed that the lattice mismatch between Si and Ge is completely accommodated by the lattice strain in the commensurate or pseudomorphic growth. To assure commensurability in the (001) plane, the lateral lattice constant of the pseudomorphic Si/Ge superlattices a_{\parallel} is then taken to be equal to that of the substrate selected as

$$a_{\parallel} = (1-x)a_{\text{Si}} + xa_{\text{Ge}}, \quad (4)$$

where $a_{\text{Si}} = 5.431 \text{ \AA}$ and $a_{\text{Ge}} = 5.658 \text{ \AA}$ are the bulk lattice constants of Si and Ge, respectively. The interplanar distances can be determined by elastic strain energy minimization. The elastic strain energy of a $(\text{Si})_4/(\text{Ge})_4$ superlattice in a tetragonal unit cell is constructed by Eq. (2). The superlattices experience a biaxial strain in the [010] and [100] directions. The elastic strain energy can be reduced both by deforming the cell tetragonally and by relaxing the interplanar spacings in the [001] direction. With x varying from 0 to 1 the interplanar spacings of a $(\text{Si})_4/(\text{Ge})_4$ superlattice is shown in Table II, where d denotes the Si-Ge interface interplanar spacing, d_1 the

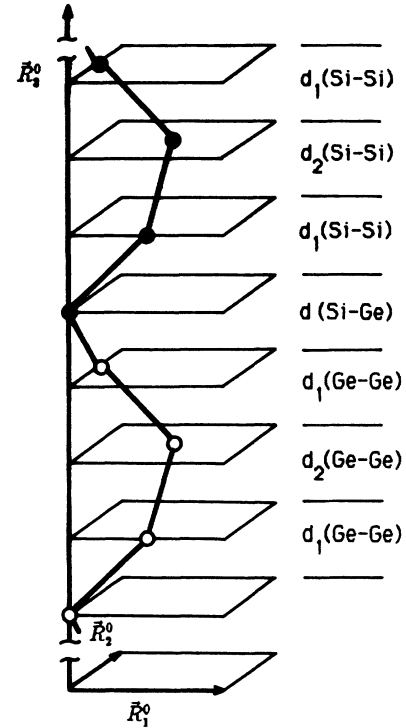


FIG. 1. Tetragonal unit cell of (001)-oriented $(\text{Si})_4/(\text{Ge})_4$ superlattice grown on a $\text{Si}_{1-x}\text{Ge}_x$ ($0 \leq x \leq 1$) substrate with solid and open circles denoting Si and Ge atoms, respectively. $\mathbf{R}_1^0 = \mathbf{R}_2^0 = a_{\parallel}/\sqrt{2}$, where a_{\parallel} is the lateral lattice constant. d denotes the interplanar spacings.

TABLE II. Interplanar spacings and lateral constants (in units of Å) for a strained $(\text{Si})_4/(\text{Ge})_4$ superlattice grown pseudomorphically on the (001)-oriented $\text{Si}_{1-x}\text{Ge}_x$ ($0 \leq x \leq 1$) substrate.

x	a_{\parallel}	$d_1(\text{Si-Si})$	$d_2(\text{Si-Si})$	$d(\text{Si-Ge})$	$d_1(\text{Ge-Ge})$	$d_2(\text{Ge-Ge})$
0.0	5.431	1.3562	1.3584	1.4075	1.4671	1.4579
0.1	5.454	1.3515	1.3537	1.4033	1.4622	1.4536
0.2	5.476	1.3468	1.3490	1.3990	1.4573	1.4494
0.3	5.499	1.3420	1.3442	1.3947	1.4524	1.4451
0.4	5.522	1.3372	1.3395	1.3904	1.4474	1.4408
0.5	5.545	1.3323	1.3346	1.3860	1.4424	1.4364
0.6	5.567	1.3274	1.3298	1.3816	1.4373	1.4320
0.7	5.590	1.3225	1.3249	1.3771	1.4323	1.4276
0.8	5.613	1.3175	1.3199	1.3727	1.4271	1.4231
0.9	5.635	1.3125	1.3149	1.3681	1.4220	1.4187
1.0	5.658	1.3076	1.3099	1.3636	1.4167	1.4142

spacing near the interface, and d_2 the spacing in the middle of the sublattice. It can be seen from Table II that the interplanar spacings vary with Ge composition factor x almost linearly. On a Si substrate ($x=0$) the Si-Si interplanar spacings are very close to those of bulk Si (1.358 Å) and the Ge-Ge spacings are expanded in comparison with their counterparts in bulk Ge (1.415 Å). On a Ge substrate ($x=1$), the Si-Si interplanar spacings are smaller than their bulk counterparts and Ge-Ge spacings are close to their bulk values. On a $\text{Si}_{1-x}\text{Ge}_x$ alloy substrate, the Si-Si spacings are contracted, whereas the Ge-Ge spacings are expanded. In any case, the Si-Ge interplanar spacings are close to the average of both sides. It is found that there exists only a small deviation between d_1 and d_2 for all values of x . On the Si side, d_1 is slightly less than d_2 , whereas on the Ge side, d_2 is smaller. These small deviations between d_1 and d_2 suggest that the strain is not uniformly distributed over the layers. With x varying from 0 to 1, the strain increases for Si layers and decreases for Ge layers. On all substrates the difference between d_1 and d_2 is no more than 0.024 Å for a Si sublattice and 0.0108 Å for a Ge sublattice. Since the value of d_1 is very close to that of d_2 , it is reasonable to neglect the deviation between d_1 and d_2 and this was what many calculations of electronic structures did.^{11,12}

For a Si substrate, the bond length of Si is found nearly the same as that of bulk Si and the bond length of Ge is very close to that of bulk Ge for a Ge substrate. However, for all values of x the Si—Si bond lengths are expanded and those of Ge—Ge are contracted. Froyen *et al.*¹⁰ suggested that the overshoot of the Si—Si bond length on the Si side of the interface and of the Ge—Ge bond length on the Ge side of the interface might cause charge transfer across the interface. Charge will flow from Si to Ge across the interface since Ge is more electronegative. The largest variations of bond lengths of Si and Ge compared with their bulk values are found to be only 1.7 and -1.6% in the case of Ge and Si substrates, respectively. These results give further support to the assumption of conservation of bond length in strained and reconstructed semiconductor layers.²³

IV. EFFECT OF SUBSTRATE ON THE GROWTH OF A $(\text{Si})_4/(\text{Ge})_4$ SUPERLATTICE

The variation of the elastic strain energy of a $(\text{Si})_4/(\text{Ge})_4$ superlattice with substrate composition factor x in a tetragonal unit cell is shown in Fig. 2. The minimum of the elastic strain energy appears at $x=0.46$, which indicates that if one selects a $\text{Si}_{0.54}\text{Ge}_{0.46}$ substrate the growth of the $(\text{Si})_4/(\text{Ge})_4$ superlattice is very close to the free standing growth. This is very meaningful to experimentalists. In Fig. 3 the strain energy distribution at each layer is plotted for $x=0, 0.46$, and 1. It is seen that for a Si substrate ($x=0$), almost all strains are taken up by the Ge layers. Whereas for a Ge substrate ($x=1$) the strains are mainly taken up by Si layers. However, for a $\text{Si}_{0.54}\text{Ge}_{0.46}$ substrate, the distribution of strains is almost symmetrical. In this case the minimum of the elastic

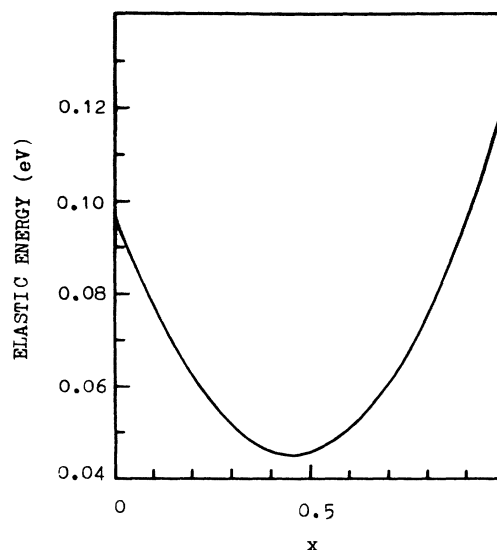


FIG. 2. The elastic strain energy of a $(\text{Si})_4/(\text{Ge})_4$ superlattice in a tetragonal unit cell.

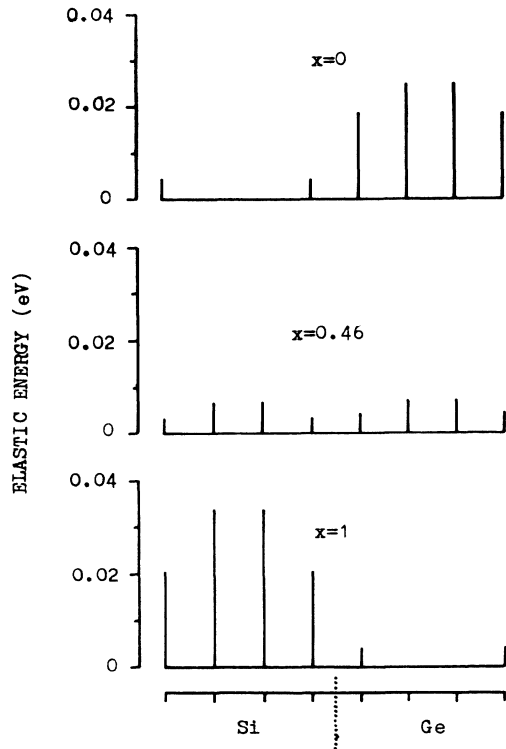


FIG. 3. The elastic strain energy distributions of a $(\text{Si})_4/(\text{Ge})_4$ superlattice for $x=0, 0.46$, and 1.

strain energy can be obtained.

The thickness of superlattices is strongly dependent on the strain distribution.⁸ The unsymmetrical strain distribution might produce an energetic instability.²⁴ On the other hand, symmetrically strained superlattices could be stable up to an unlimited overall thickness. In order to have a larger $(\text{Si})_4/(\text{Ge})_4$ superlattice thickness, the present results indicate that an appropriate $\text{Si}_{0.54}\text{Ge}_{0.46}$ substrate is suggested. In this case the symmetrically strained superlattices can be obtained.

V. VIBRATIONAL PROPERTIES OF A $(\text{Si})_4/(\text{Ge})_4$ SUPERLATTICE

Vibrational properties of Si/Ge superlattices are extensively studied both experimentally²⁻⁸ and theoretically.¹³⁻¹⁵ To our knowledge, there are no lattice-dynamics calculations of Si/Ge superlattices which take strain into account. Under the results obtained in the above sections, lattice dynamics of a strained $(\text{Si})_4/(\text{Ge})_4$ superlattice grown on a (001)-oriented $\text{Si}_{1-x}\text{Ge}_x$ substrate can be studied. In the calculations the long-range (Coulomb) interactions are neglected. This does not affect results substantially since the Si—Ge bonds are almost homopolar. The calculations are performed only for phonons propagating in the [001] growth direction, however in the same framework, phonons in other directions can also be calculated. The effect of strain is also considered in our calculations. The Keating parameters used in this section are the same as shown in Table I and Eq. (3). The structural configurations of $(\text{Si})_4/(\text{Ge})_4$ superlattices are

taken from the above section. The force constants between two atoms can be obtained directly by differentiating the elastic strain energy from Eq. (2). The force-constant matrix element $\Phi_{\eta\eta'}(s,s')$ between atoms s and s' is given by

$$\Phi_{\eta\eta'}(s,s') = \frac{\partial^2 E}{\partial u_{\eta}(s) \partial u_{\eta'}(s)}, \quad (5)$$

where η and η' denote Cartesian coordinates and $u_{\eta}(s)$ is a small displacement of atom s from its equilibrium position along the η direction. The elastic strain energy E is obtained from Eq. (2). The force constant is composed of a bond-stretching and bond-bending contribution.

The calculated phonon dispersion curves along the [001] direction for $(\text{Si})_4/(\text{Ge})_4$ superlattices grown pseudomorphically on a Si(001) substrate (corresponding to $x=0$) are given in Figs. 4 and 5. For comparison, in Fig. 4 the phonon dispersion curves in longitudinal polarizations calculated by Alonso *et al.*¹⁵ are also plotted. It can be seen from Fig. 4 that there exist some differences

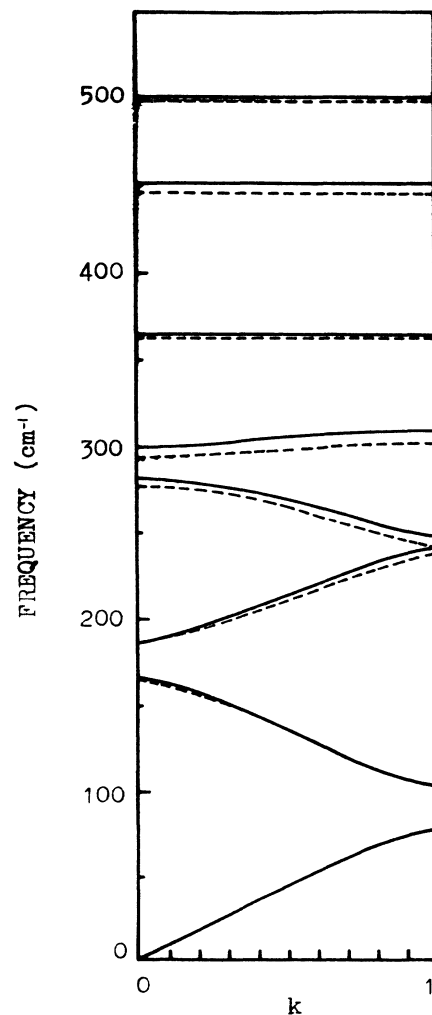


FIG. 4. Phonon dispersion curves of the L mode ([001]-polarized) along the [001] direction for $(\text{Si})_4/(\text{Ge})_4$ superlattice grown on a Si substrate ($x=0$). The solid curves are the present results and dashed curves are given by Alonso *et al.* (Ref. 15).

of phonon frequencies between the present results and those of Alonso *et al.*¹⁵ since in our calculations strain effect is taken into account. In addition, the difference in the choice of Keating parameters $\beta(\text{SiGeSi})$, $\beta(\text{SiGeGe})$, and $\beta(\text{SiGeSi})$ might also affect the results. In Figs. 6–8, the calculated phonon frequencies and displacement patterns as a function of x are shown for a $(\text{Si})_4/(\text{Ge})_4$ superlattice at the zone center in the [001] polarization (longitudinal), [100] polarization (transverse), and [010] polarization (transverse), respectively. It is found that the displacement patterns remain unchanged with the variation of x . The modes are numbered in the order of increasing frequencies. Mode 1 corresponds to the zero frequency mode. For the longitudinal (L) mode, the phonon frequencies decrease almost linearly with the increase of x , however for the transverse (T) modes the frequencies increase linearly. This can be understood by the fact that the presence of strain in Si/Ge superlattices causes the lattices to distort both in the in-plane and growth directions, which produces a linear shift of phonon frequen-

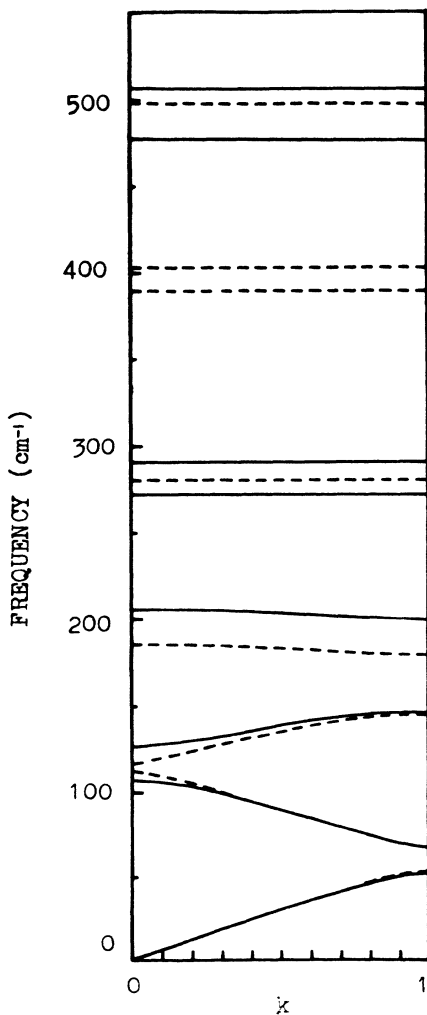


FIG. 5. Phonon dispersion curves of [100]-polarized T_1 (solid lines) and [010]-polarized T_2 (dashed lines) modes along the [001] direction for a $(\text{Si})_4/(\text{Ge})_4$ superlattice grown on a Si substrate ($x=0$).

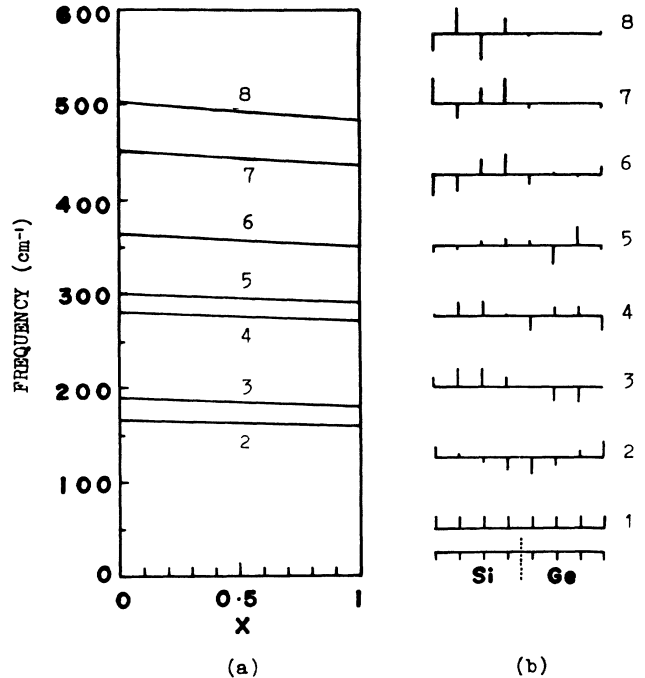


FIG. 6. (a) L mode ([001]-polarized) phonon frequencies of a $(\text{Si})_4/(\text{Ge})_4$ superlattice at the zone center; (b) typical displacement patterns of L modes.

cies.²⁵ The changes of phonon frequencies with the change of x are more significant for high-frequency modes.

The L modes in Fig. 6 are [001]-polarized. Modes 6–8 are the typical Si-like confined LO modes with vibrational amplitudes mainly in Si layers. Since the frequency of

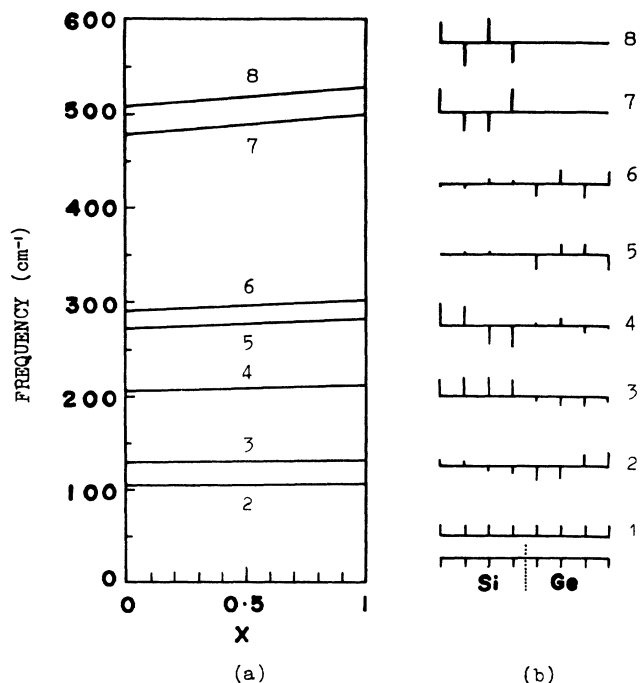


FIG. 7. (a) T_1 mode ([100]-polarized) phonon frequencies of a $(\text{Si})_4/(\text{Ge})_4$ superlattice at the zone center; (b) typical displacement patterns of T_1 modes.

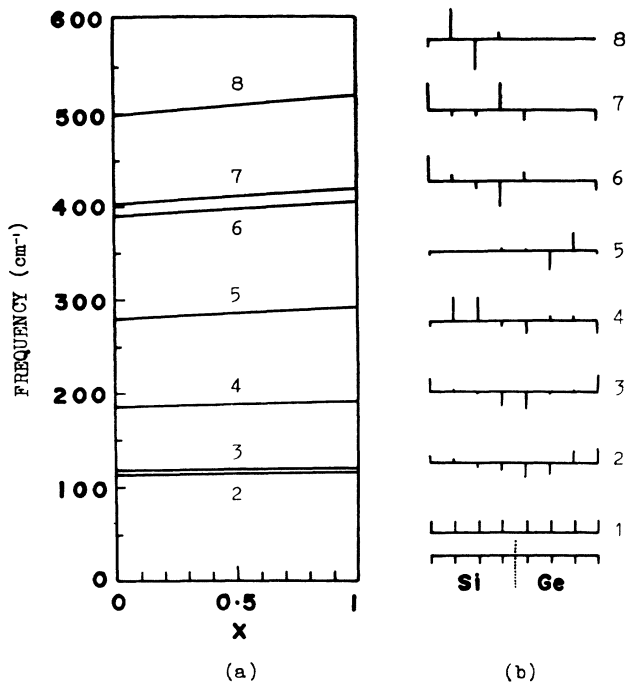


FIG. 8. (a) T_2 mode ([010]-polarized) phonon frequencies of a $(\text{Si})_4/(\text{Ge})_4$ superlattice at the zone center; (b) typical displacement patterns of T_2 modes.

mode 5 overlaps with the bulk continuum of Si and Ge, this mode is a resonant, quasicontained Ge-like LO mode with vibrational amplitudes localized mainly at Ge layers. Modes 1–4 are the mixed modes resulting from the folding of the LA modes of Si and Ge. It was observed in Raman-scattering experiments that there exist three main peaks around 500, 400, and 300 cm^{-1} , which are currently attributed to Si, Si-Ge, and Ge modes, respectively. In our calculations there are modes around 500 and 300 cm^{-1} corresponding to confined Si-like and Ge-like modes, respectively. However, no interface modes around 400 cm^{-1} are found. The interface modes around 400 cm^{-1} in the longitudinal polarization are also not found in the calculations carried out by other authors.^{13–15} Molinari *et al.*¹³ concluded that interface Si-

Ge modes around 400 cm^{-1} cannot exist in the longitudinal modes unless some alloying at the interface is introduced.

It is worthwhile to note that mode 2 is really an interface mode resulting from the first folding of the LA mode. This mode can be observed in the $Z\bar{Z}$ scattering geometry by Raman scattering.

The T_1 modes in Fig. 7 are [100]-polarized. Modes 7 and 8 are Si-like confined TO modes, modes 5 and 6 Ge-like quasicontained resonant TO modes, and mode 4 Si-like confined TA mode. Mode 2 is an interface TA mode.

The T_2 modes in Fig. 8 are [010]-polarized. Mode 8 is a Si-confined TO mode and mode 5 a Ge-like quasicontained resonant TO mode. Between modes 8 and 5, proper interface modes appear (modes 6 and 7) with frequencies around 400 cm^{-1} . Modes 2 and 3 are found to be interface TA modes.

VI. DISCUSSION AND CONCLUSION

The structural and vibrational properties of a [001]-oriented $(\text{Si})_4/(\text{Ge})_4$ superlattice grown on $\text{Si}_{1-x}\text{Ge}_x$ ($0 \leq x \leq 1$) substrates are obtained by the present calculations. Moreover, variations of interplanar spacings with different substrates are also given.

For a $\text{Si}_{0.54}\text{Ge}_{0.46}$ substrate, the minimum of the elastic strain energy is obtained and the strain distribution is almost symmetrical, which indicates that on this substrate the growth of a $(\text{Si})_4/(\text{Ge})_4$ superlattice is preferable. It is hoped that some evidence for this conclusion will be given in the near future.

In the lattice-dynamical calculations, the lattice strains are taken into consideration. Thus, the results obtained should be more reasonable than those obtained previously. The results show that with increasing x , frequencies of L modes decrease almost linearly, whereas that of T modes increase linearly. It is found that among L modes the topmost one around 500 cm^{-1} is a Si-like confined LO mode and the mode around 300 cm^{-1} is the Ge-like quasicontained resonant LO mode. These are in good agreement with experiment. No interface modes around 400 cm^{-1} are found in [001] polarization in our calculations. However, interface modes with frequencies around 400 cm^{-1} are present in the [010] polarization.

¹G. C. Osbourn, J. Appl. Phys. **53**, 1586 (1982); T. P. Pearsall, F. H. Pollak, J. C. Bean, and R. Hull, Phys. Rev. B **33**, 6821 (1986).

²E. Friess, H. Brugger, K. Eberl, G. Krotz, and G. Abstreiter, Solid State Commun. **69**, 899 (1989).

³J. Berk, A. Ourmazd, L. C. Feldman, T. P. Pearsall, J. M. Bonar, B. A. Davidson, and J. P. Mannaerts, Appl. Phys. Lett. **50**, 760 (1987).

⁴J. Berk, J. P. Mannaerts, L. C. Feldman, B. A. Davison, and A. Ourmazd, Appl. Phys. Lett. **49**, 286 (1986).

⁵W. Bacsa, H. v. Kanel, K. A. Mader, M. Ospelt, and P. Wachter, Superlatt. Microstruct. **4**, 717 (1988).

⁶S. J. Chang, C. F. Huang, M. A. Kallel, K. L. Wang, R. C. Bowman, Jr., and P. M. Adams, Appl. Phys. Lett. **53**, 1835 (1988).

⁷T. P. Pearsall, J. Berk, L. C. Feldman, J. M. Bonar, J. P. Mannaerts, and A. Ourmazd, Phys. Rev. Lett. **58**, 729 (1987).

⁸E. Kasper, H. Kibbel, H. Jorke, and H. Brugger, E. Friess, and G. Abstreiter, Phys. Rev. B **38**, 3599 (1989).

⁹K. B. Wong, M. Jaros, I. Morrison, and J. P. Hagon, Phys. Rev. Lett. **60**, 2221 (1988).

¹⁰Sverre Froyen, D. M. Wood, and Alex Zunger, Phys. Rev. B **36**, 4547 (1987); **37**, 6893 (1988).

¹¹S. Ciraci and Inder P. Batra, Phys. Rev. B **38**, 1835 (1988).

¹²S. Satpathy, R. M. Martin, and C. G. Van de Walle, Phys. Rev. B **38**, 13 237 (1988).

¹³E. Molinari and A. Fasolino, Appl. Phys. Lett. **54**, 1220 (1989); A. Fasolino and E. Molinari, J. Phys. (Paris) Colloq. **48**, C5-569 (1987).

¹⁴A. Fasolino, E. Molinari, and J. C. Maan, Phys. Rev. B **39**,

- 3923 (1989).
- ¹⁵M. I. Alonso, M. Cardona, and G. Kanellis, *Solid State Commun.* **69**, 479 (1989).
- ¹⁶P. N. Keating, *Phys. Rev.* **145**, 637 (1966).
- ¹⁷R. M. Martin, *Phys. Rev. B* **1**, 4005 (1970).
- ¹⁸J. S. Pedersen, *Surf. Sci.* **210**, 238 (1989).
- ¹⁹J. A. Appelbaum and D. A. Haman, *Surf. Sci.* **74**, 21 (1978).
- ²⁰R. M. Tromp, *Surf. Sci.* **155**, 432 (1985); R. M. Tromp and E. J. van Loenen, *ibid.* **155**, 441 (1985).
- ²¹T. Yamaguchi, *Phys. Rev. B* **30**, 1992 (1984); **31**, 5297 (1985); **32**, 2356 (1985).
- ²²J. Zi and K. M. Zhang, *Chin. J. Comput. Phys.* **6**, 67 (1989).
- ²³D. J. Chadi, *Phys. Rev. Lett.* **43**, 43 (1979).
- ²⁴E. Kasper, H. -J. Herzog, H. Dambkes, and G. Abstreiter, in *Layered Structures and Epitaxy*, Vol. 56 of *Materials Research Society Symposia Proceedings*, edited by M. Gibson, G. C. Osbourne, and R. M. Tromp (MRS, Pittsburgh, 1986), p. 347.
- ²⁵F. Cerderia, A. Pinczuk, J. C. Bean, B. Batlogg, and B. A. Wilson, *Appl. Phys. Lett.* **45**, 1138 (1984).